





# EXPERIMENTAL ROBOT MODEL ADJUSTMENT BASED ON FORCE-TORQUE SENSORS INFORMATION

Santiago Martinez <sup>1\*</sup> , Juan Miguel Garcia-Haro <sup>1</sup> , Juan G. Victores <sup>1</sup> , Alberto Jardon <sup>1</sup>   
and Carlos Balaguer <sup>1</sup> 

<sup>1</sup> Universidad Carlos III de Madrid, Avd. Universidad, 30, Leganés, Madrid, Spain

\* Correspondence: scasa@ing.uc3m.es; Tel.: +34-91-624-5997

Version March 6, 2018 submitted to Sensors

**Abstract:** The computational complexity of humanoid robot balance control is reduced by means of applying simplified kinematics and dynamics models. But these simplifications lead to introduce errors that are added to other inherent electro-mechanic inaccuracies that affect to the robotic system. Linear control systems deal with these inaccuracies if they operate around an specific working point but are less precise if not. This work presents a model improvement based on the Linear Inverted Pendulum Model (LIPM) to be applied in a non-linear control system. The aim is to minimize the control error and reduce robot oscillations for multiple working points. The new model, named Dynamic LIPM (DLIPM), is used to plan the robot behavior against changes in the balance status denoted by the Zero Moment Point (ZMP). Thanks to the use of the information of Force-Torque sensors, an experimental procedure has been applied to characterize the inaccuracies and introduce them in the new model. The experiments have consisted of balance perturbations similar to push-recovery trials, in which step shaped ZMP variations are produced. The results show that the response of the robot against balance perturbations are more precise and the mechanical oscillations are reduced without comprising the robot dynamics

**Keywords:** Force-Torque sensors, balance control, humanoid robot, simplified model

## 1. INTRODUCTION

In robotics, the most versatile but complex machines are humanoid robots. Their complex mechanical structure, high number of Degrees of Freedom (DOF) and, control requirements favor the seeking for simplifications that enable the deployment of multiple tasks. Human-like or humanoid robots are designed for working in scenarios in the same way than humans do, but they have nowadays very serious limitations performing tasks. For instance, working in manufacturing plants in which heavy parts must be processed, disaster scenarios, service applications, etc. In such situations the need for interaction with the surrounding environment is always present. Humanoid robots, physically similar to human beings, must fulfill a very important requirement: the robot must be able to move around its environment keeping balance.

When a humanoid robot performs tasks and walks through plain, rough or sloped terrains it has to be ensured that the robot will not fall over [1][2]. Even if there are obstacles placed in the robot environment and path re-planing is required [3][4], normal step pattern must be changed always maintaining stability. Furthermore, previous to walking pattern generation, robot joints constraints, dynamic parameters (velocities, accelerations, etc.), and joint torques [5] have to be observed in real time to not overload the system and make the walking task viable.

In the case of human beings presence, unexpected disturbances can appear due to intentional or accidental interactions. In this situation the robot is actuated by an external force and the robot must

34 counteract it to recover its balance status and prevent a falling [6][7]. A more complex situation comes  
35 when the robot is carrying an object itself or collaborating with a human [8]. An unknown weight  
36 has to be considered and the system model is completely different, taking the object as a part of its  
37 body. Each one of these situations lead to the use of one particular model of the robot which takes into  
38 account different requirements from the surrounding environment, the mechanical distribution of the  
39 robot itself, etc.

40 Their complex mechanical structure, high number of Degrees of Freedom (DOF) and, control  
41 requirements favor the seeking for simplified models that enable the deployment of multiple tasks.  
42 But the use of these models lead to the amplification of inherent inaccuracies of the humanoid robot  
43 system. The concept of "simplified model" implies the assumption of errors to favor other aspects such  
44 as computing velocity, controllability, etc. The simplest model of a humanoid robot used in balance  
45 control is the inverted pendulum. It represents the location and movement of the Center of Mass  
46 (CoM) of the robot, which pivots around a support base thanks to a rotating joint. Due to its simplicity,  
47 its easy to state that many inaccuracies are introduced and system features are omitted. For instance,  
48 the location at any time of the CoM depends on the robot posture and may not be coincident with the  
49 location represented by an pendulum model with an specific and fixed configuration.

50 Many improvements and new models have been developed to add more information about the  
51 robot body or to solve lack of information, such as in [9][10]. As well, these new models can represent  
52 special behaviors or modeling special tasks [11][12]. This paper presents one of those improvements for  
53 dealing with the robot inaccuracies such as material flexibility or component tolerances that are very  
54 difficult to be modeled. System inaccuracies have been quantified and studied to model experimentally  
55 the robot response. Then, these errors has been modeled and, finally, it has been reduced their effects  
56 by introducing a counteracting action within a pendulum model, as will be described in following  
57 sections. By means of an error scheduling method, the model parameters for control can be dynamically  
58 computed. This can be established as a methodology that can be applied to other robot control tasks.  
59 The experimental platform used in this work is the humanoid robot TEO (*Task Environment Operator*)  
60 from University Carlos III of Madrid [13], shown in Fig. 1.

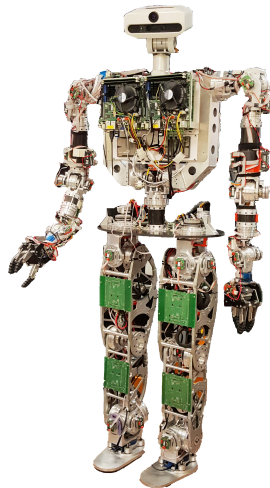


Figure 1. TEO Humanoid Robot from University Carlos III of Madrid.

## 61 2. BACKGROUND

62 To solve complexity, the humanoid robot is usually represented by means of simplified models  
63 that enable an easy way of designing controllers. These models represents kinematics and dynamics  
64 of the robotic system in action. Taking in account different parameters of the robot, such as the mass,  
65 the location of its CoM, inertia tensors, etc. many approximate models of the robot for each task

context can be established. This work is focused in the study of simplified models applied in balance control and how inherent model errors can be overcome to improve robot operation. This background is mainly divided in the enumeration of some simplified models and how they are used in balance control.

### 2.1. Robot Simplified models

The simplest model for representing robot's kinematics and dynamics is the two dimensional inverted pendulum with one or two DoF [14]. These models represent a concentrated CoM linked rigidly to the ground by one rotational joint like in Fig. 2 left, or including a linear joint like in Fig. 2 right.

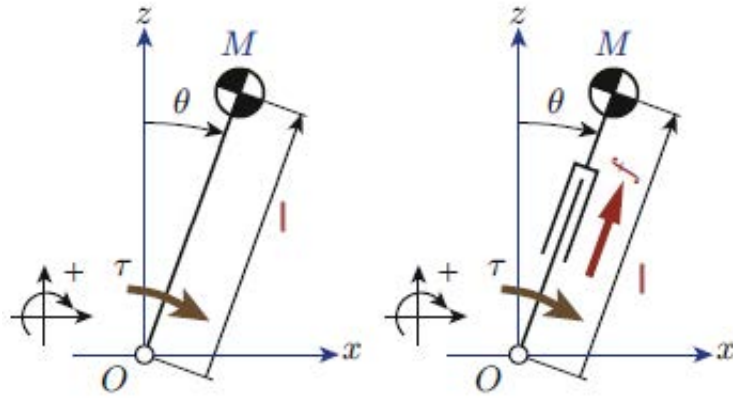


Figure 2. Basic Inverted Pendulum Models in x-z plane. 1 DoF (left) and 2 DoF (right).

In the case of Fig. 2 left, the movement of the CoM is defined by the following equation:

$$\tau = -ml^2\ddot{\theta} + mgl \sin \theta \quad (1)$$

where  $m$  is the mass of the CoM,  $l$  the pendulum longitude,  $\tau$  the torque at the pivot point and  $\theta$  is the pendulum angle. But this is a non-linear equation that makes its implementation in a robot controller more difficult. To overcome this problem it is assumed that  $\theta$  is small enough to consider  $\sin \theta = \theta$ . Then, the resulting model is one of the most famous models used in humanoid robotics. It is the Three Dimensional Linear Inverted Pendulum (3DLIPM) shown in Fig. 3 and proposed by Kajita [15].

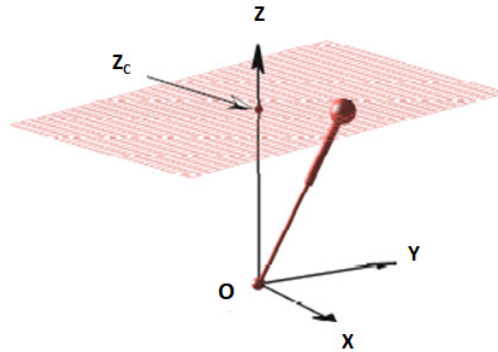


Figure 3. 3DLIPM Model [14].

Then, Eq. (1) becomes (for 2D case in plane x-z):

$$\tau = -ml^2\ddot{\theta} + mgl\theta \quad (2)$$

with the z-coordinate movement constrained to an horizontal plane (Fig. 3):

$$z = z_c \quad (3)$$

The main advantage of 3DLIPM is the linear equations that are very easy to program in a computer. They are mainly used for walking pattern generation and balance control. The application of this equation for balance control is possible whether ground reaction (vertical force) and torques in the robot's ankle joint, which correspond with the point  $O$  of the model, can be measured. It has been achieved by the use of Force-Torque (F-T) sensors at ankle level, such as JR3 sensors assembled in robot TEO feet (Fig. 4).



**Figure 4.** TEO's ankle joints with JR3 F-T sensor.

But 3DLIPM does not provide information about body accelerations and inertias, that are very useful information for a biped robot during a dynamic walking task. This issue was solved with the development of the Cart-Table simplified model (Fig. 5). In this case, the information need by the model is provided by Inertial Measurement Units (IMUs) which sense velocities and accelerations of the robot body.

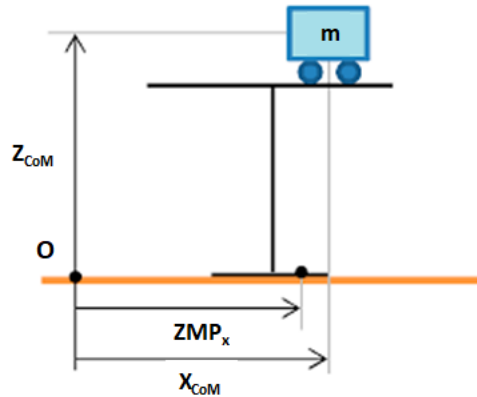


**Figure 5.** Cart-Table simplified model.

Cart-Table and 3DLIPM are the most used simplified models in balance control. Nevertheless, other researchers lead their works towards multi-link models, where they use a precise knowledge about dynamics of each robot link [16][17].

## 2.2. Zero Moment Point and balance

The study of humanoid robots balance has been supported by the simplified models described before. Many tools have been developed to describe the kinematic and dynamic behavior of a humanoid when it performs tasks. Taking in account that one of the main goals of a humanoid robot is to achieve stable walking behaviors, these tools have been widely studied in this field.

The development of a humanoid balance control architecture is mainly related to the study of two specific reference points. The first one is the Center of Mass used to model humanoid body as described in the previous subsection. But CoM does not provide useful information about the body balance status. Zero Moment Point (ZMP) introduced by Vukobratovic in [18] is the first and the main tool developed for describing body's equilibrium. The ZMP was defined firstly as the point in the support base, usually the ground, where the resulting torque caused by all forces exerted over the robot's body is equal to zero. Fig. 6 illustrates the ZMP location  $P$  and Eq. (4) defines it mathematically.

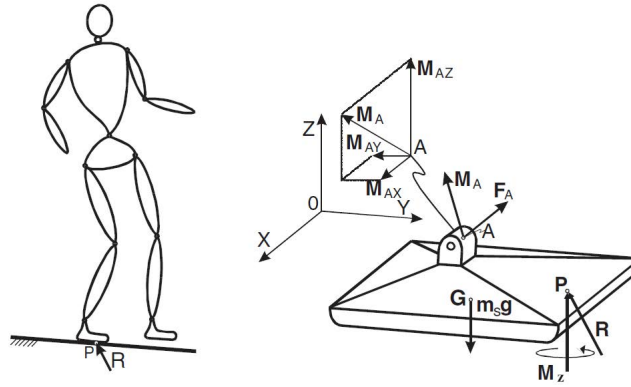


Figure 6. ZMP ( $P$ ) location [18].

$$P_x = -\frac{\sum x \cdot F_z}{\sum F_z} \quad (4)$$

In Eq. (4), for the coordinate  $x$ , the sum of the torques produced by the mass of each link of the body due to gravity is divided by the sum of reaction forces. For an static posture, if the value of ZMP coordinate lays inside the support polygon of the robot, the balance of the robot can be guaranteed. But when the ZMP is in the edge of the support area, the humanoid body can loose balance and fall down.

The computation of the ZMP depends on the posture of the robot and the location of the CoM of each limb. Due to that, ZMP calculation gains the advantage of representing the robot body as a simplified model for two main reason. The first one is the simplicity of the equations used for ZMP computation. The second reason is the possibility of using F-T sensors to measure all the forces and torques need for ZMP computation. The model applied in this work is the 3DLIPM modified to match with the TEO robot structure, as can be observed in Fig. 7.

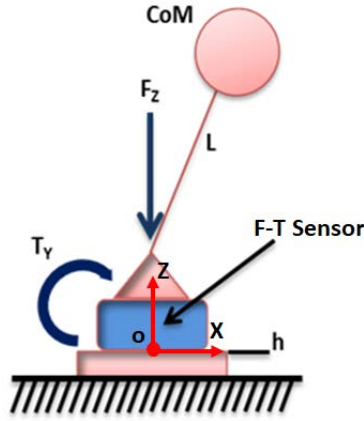


Figure 7. LIPM with F-T sensor between sole and ankle joint.

When a biped robot is supporting its body on one foot, the robot ankle is considered the pivot point connected to the robot's CoM by means of a massless leg. The simplest model only considers the gravitational force exerted to the mechanism and the pendulum motion is represented by Eq. (2). According to [19], the ZMP equation in the sagittal plane obtained from the LIPM when the robot is standing on one foot:

$$x_{ZMP} = -\frac{\tau_y + hF_x}{F_z} \quad (5)$$

where  $\tau_y$  is the torque at the pivot point around  $y$  axis,  $F_x$  is the measured force in the  $x$  direction and  $h$  is the distance from the ground to the location of the sensor (generally the sole height). But when the robot stands in double support (both feet lie on the ground), ZMP obtained from each foot is used to compute the global ZMP [14]:

$$x_{ZMP_{DS}} = -\frac{x_{ZMP}^R \cdot F_z^R + x_{ZMP}^L \cdot F_z^L}{F_z^R + F_z^L} \quad (6)$$

where upper index  $R$  represents the right foot and  $L$  the left one. Even when the robot is in double support-phase and two pivot points at the ankle joints exist, the inverted pendulum can be used. If the movement is in the sagittal plane, the robot behaves as a single inverted pendulum because both ankles have the same movement along the  $x$  axis.

### 2.3. Balance control

One of the main skills defining the human being is the capacity of walking upright. In the same manner, this is one of the main features that a humanoid robot must to achieve. The key question relays on the balance of the upright posture to avoid falls, during a walking task or standing still. The use of the simplified models of the body and tools such as ZMP enables the deployment of stabilizers to maintain equilibrium.

Before performing a walking task, the humanoid robot must to keep an upright stable posture. In this situation, the robot must deal with unexpected disturbances as the first premise to develop a balance control architecture. So, achieving this upright stable posture is the first stage to develop an stabilizer. One of the main techniques to start the development of a balance control architecture is based on push-recovery experiments, like shown in Fig. 8. The robot must deal with unexpected disturbances represented as forces applied to it. If unexpected disturbances appear and depending on the intensity level of the disturbance, different control strategies can be set [20]: ankle, hip and step strategy. For low intensity disturbances, the body can be considered as a nearly single stiff pendulum, where balance adjustments are mainly made in the ankle joints of the robot [12]. The hip

strategy is applied when the external disturbance increases and the ankle strategy is not enough to keep balance. When acting this strategy, the robot can move its hip independently or in combination with the ankle strategy. Then, the robot model has to be modified, considering a double inverted pendulum [20][21]. The double inverted pendulum consists of an upper link and a lower link, which involves that each single pendulum has an influence on the other one. Step strategy is only used when postural corrections become insufficient and the base of support must be adjusted. Taking this in account, the very beginning phase to develop an stabilizer is to deploy the control system for each strategy, starting from the ankle one.

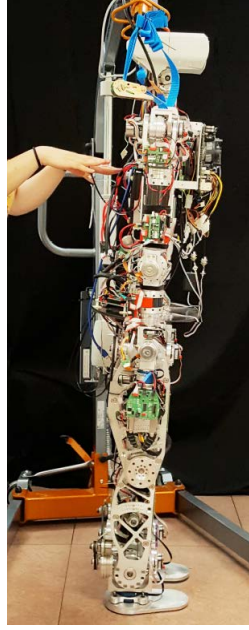


**Figure 8.** Experiment applying a force to the robot TEO.

Balance control with the ankle strategy concept is applicable both to standing in upright posture and, as well, to walking tasks. In both situations, the robot is modeled as an inverted pendulum. The disturbance is a force applied to the CoM of the model. This force can lead the ZMP to be out of the support polygon and the robot would loose balance. Then, the robot must counteract this disturbance applying a torque in the ankle joints, trying to maintain ZMP inside the support area. This kind of control is called *ZMP control by ankle torque* [22][23]. Finally, the ankle's torque is transformed into angle commands  $\theta = f(\tau)$  and they are send to the robot. This is represented by the control architecture depicted in Fig. 9.

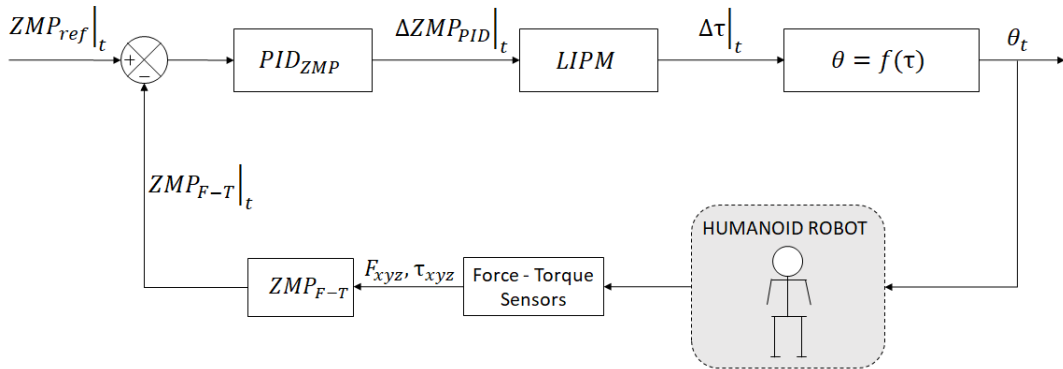


**Figure 9.** Basic ZMP position controller using LIPM model.



But traditional PID Control relies on the proper the proper selection of values to be used for the Proportional (P), Integral (I), and Derivative (D) constants for a linearized working point [24]. If the process is non-linear, the control designer must then continuously evaluate it and tune the constants. Instead using PID controllers, Model-Based Controllers are able to learn how a process responds to changes, and in turn, they can automatically make the tuning adjustments that would traditionally be manual.

### 3. PROBLEM STATEMENT

However, there are many errors that the balance control system must deal with. Simplified model control approaches always introduce errors. Pendulum mathematical model is not linear, but ZMP equations are obtained from a linear pendulum. When the angle of the pendulum is small enough, it is assumed that  $\sin \theta = \theta$ , which introduces an error to the system. The mass of the Center of Gravity (CoG) is also an approximated value of the whole robot mass, even its location can change. Joining all this assumptions, errors in the system become remarkable.

Also, there can be measurement deviations in the Force-Torque (F-T) sensors due to calibration errors, or in analogue to digital data conversions. Other systematic errors as the flexibility of the structure (due to the height of the robot), loosenesses between mechanical parts (as transmissions or unions of pieces), and small irregularities in the ground are usually not considered. All of these errors lead to increase the control effort and makes the control tuning task more difficult.

The aim of this work is to improve the ZMP control system described in Fig. 9, proposing an Dynamic LIPM (DLIPM). This model will include the errors depicted in Fig. 10 and more. The procedure to model this error is based on push-recovery experiments in which the ZMP is computed thanks to the measures provided by F-T sensors. Then, the real ZMP is compared with the planned ZMP, obtaining the error. Finally, the error is introduced in the model as a fictitious force that modifies the inverted pendulum model behavior.

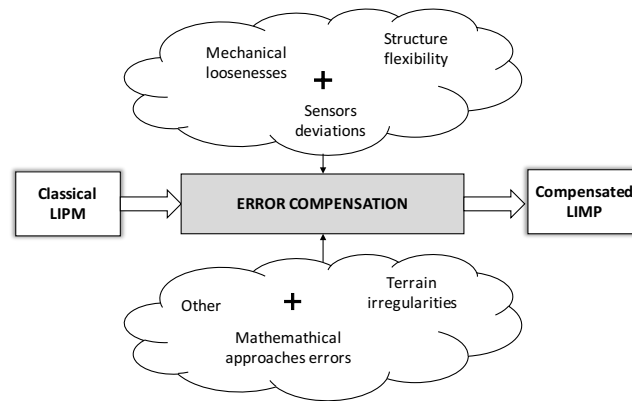


Figure 10. Error compensation diagram.

From the control point of view, real humanoid mechanisms are slightly flexible [22]. Usually the flexibility is close related to the robot height and, although robot designers try make stiff structures, it is impossible to eliminate it. Because of this compliance, the humanoid robot exhibits the characteristics of a lightly damped structure. For example, in a static case when the ankle joint is under position control, a pushing external force can easily excite an oscillation. This oscillation exists even when the position error in every joint is zero. As well, there are other error sources that have influence in the correlation of the robot with model (Fig. 10). But it is very difficult to identify and define these errors mathematically.



The existence of these errors have high influence on the ZMP computation and, for that, on the balance control system. Fig. 11 illustrates how robotic system inaccuracies and other error sources affects to the location of the ZMP. In this example,  $u$  denotes the model angle expected caused by the commanded joint torque. The expected ZMP would be represented by  $x_{exp}$ . If we consider only the error introduced by the robot flexibility, the ZMP location would be the one represented by  $x_{err}$ . Nevertheless, the real ZMP computed using the forces and torques measured is  $x_{F-T}$ .

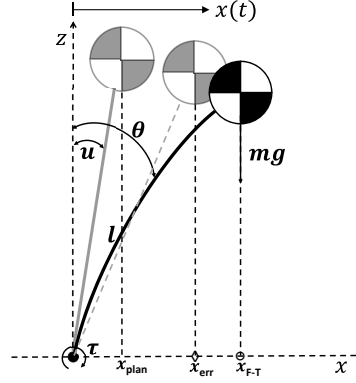


Figure 11. Single inverted pendulum model including robot's flexibility [22].

Then, the problem is the mismatch between the ZMP expected or planned and the real ZMP measured with the F-T sensors. In order to reduce this gap, this work propose a model improvement closer to the real robot behavior. Furthermore, ZMP control architecture for keeping balance can be as well improved.

#### 4. METHODS AND EXPERIMENTAL PROCEDURE

To achieve it, the error has been modeled using the information of the F-T sensors installed in the ankles of the robot. All the effects caused by any disturbance are reflected in the forces and torques measured by the sensors. In this way, it is necessary to separate the information related to the inaccuracies and the other related to the expected behavior. Two assumptions need to be made before performing this procedure. The first one is the necessity of establishing the inverted pendulum model parameters: CoM location and mass. They come from the robot design but they are not complete accurate because differences between CAD designs and real implementation. The correction of this parameters using the real robot is not possible, so it is assumed the use of the theoretical values. The second assumption is related to the planning of balance control task. Taking into account the established model, ZMP location can be planned. That is, ZMP location can be pre-planned to remain always inside the support polygon. It is desirable that balance plan will be close to reality in order to reduce the effort of the control system. This means that lower gains will be need to adjust the control system.

The method used to develop the new improved model is the following; based on open-loop system push-recovery set of experiments, the measurements of the F-T sensors are captured and processed. Then, with this information, ZMP real  $x_{F-T}$  is computed and compared with ZMP expected  $x_{exp}$ . The difference between them is modeled and one equation describing this error is obtained. The modeled error is included in the original model as a fictitious force that corrects the difference found. Once the new model has been obtained, the new planned ZMP behavior is close to the ZMP measured.

##### 4.1. Study of the system response

To introduce into TEO simplified model all the errors mentioned before, the procedure summarized in Fig. 12 has been followed. This procedure has been divided in three phases:

experimental, data analysis and validation of results. This procedure has allowed to obtain a set of data from the F-T sensors to be used in the generation of the new custom model.

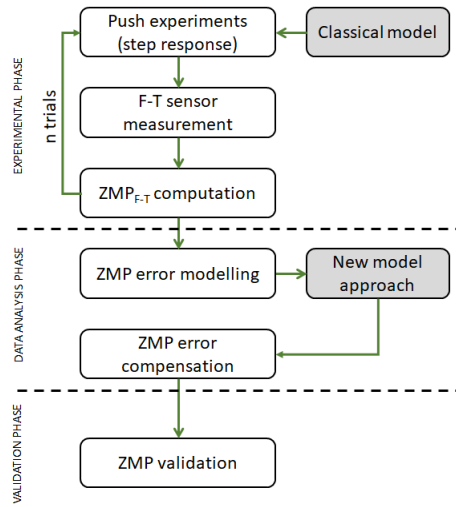


**Figure 12.** Experimental procedure diagram.

The first stage of the procedure is to fix the inverted pendulum model parameters with the characteristics of the humanoid robot TEO. The robot weight is 62.6 kg and the height from the ground to the CoM is 0.893 m (the pendulum length). Then, it has been experimented the movement of the robot caused by a pushing force. The effect of this force is a variation of the ZMP location depending the its intensity. It is important to remark that the robot doesn't keep the initial value of ZMP during each experiment, that is, it doesn't recover the initial posture. This behavior is similar to the study of the response of a system with an step angular input in the ankle joint. After a set of trials, the ZMP error has been modeled as the difference between the expected and the measured value. As well, the dynamic behavior of the ZMP variation has been studied. The last phase of this procedure has consisted of the validation of the new model within the new control architecture.

To illustrate the method only the results from the saggital plane (x-z) of the robot are presented because the experimental methodology for the frontal plane (y-z) is the same and similar results has been obtained. This study and methodology is extensible to any other spatial direction. In this way, the experimental setup is represented by Fig. 13. The robot is in a flat ground environment with both feet on the ground (double support). Therefore, the support area includes the robot footprints and the common tangents between them.

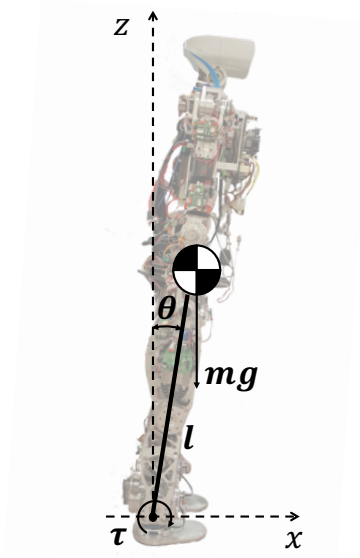


Figure 13. Experimental setup of TEO robot.

After performing a set of trials, the results are shown in Fig. 14. This figure represents the ZMP measured (the oscillating signals) and the expected ZMP (the step form signals). Each pair of ZMP signal (oscillating-step) correspond to a specific pushing force applied to the robot. If we examine each pair, some conclusions can be extracted. Bigger disturbances imply further location of the ZMP from its origin, making the robot more unstable because ZMP is closer to the support polygon edge. It means that the angle from the model, that is commanded to the robot, is bigger and the errors have more influence, mainly robot flexibility and mechanical tolerances. For this reason, the steady state error is as well higher. Furthermore, the system have a higher initial oscillating response, which is not desirable when ZMP is located near the edge of the support polygon.

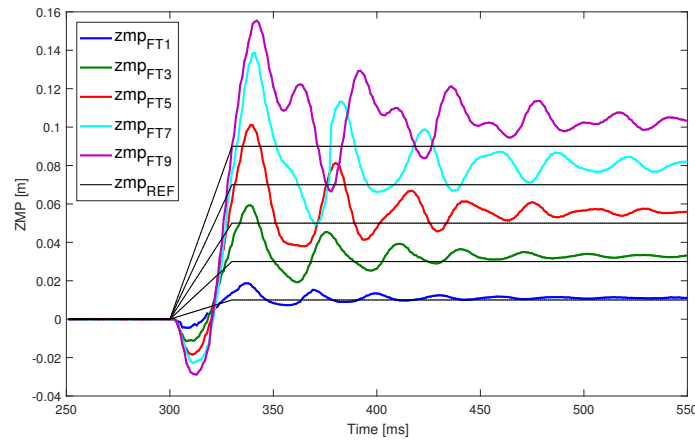
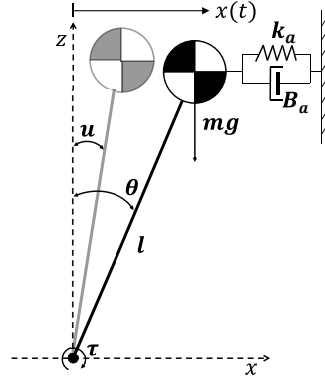


Figure 14. Step response experiments.

This dataset is the base for developing an improved ZMP control without the necessity of low level position or torque controller parameters tuning. The objective of next steps is to obtain a transfer function modeling the ZMP behavior. The resulting transfer function, that models ZMP deviations, will be added to the classic LIPM with two main purposes: the elimination of steady state error and the reduction of transient oscillation and overshooting.

#### 4.2. Dynamic linear inverted pendulum model

To accomplish the ZMP control requirements (settling time and overshoot level), this work proposes an improvement model derived from the classic LIPM. The objective is to modify the initial model adding a system that represents the errors of the real robot obtained from experimentation. Then, balance parameters measured will have less deviation from planned and the control response can be reduced. Fig. 15 represents the complete model in which a spring  $k_a$  and a damper  $B_a$  have been added to the initial inverted pendulum model. These mechanical model try to compensate the steady state response ( $k_a$ ) and the transient response to limit oscillations ( $B_a$ ).



**Figure 15.** Proposed compensated inverted pendulum model.

Then, the equation of motion of the model shown in Fig. 15 is given by:

$$\tau = -ml\ddot{x}(t) - B_a l\dot{x}(t) - k_a l x(t) + mgx(t) \quad (7)$$

where  $x(t)$  is the CoM movement,  $m$  is the pendulum mass located at the CoM,  $l$  its longitude,  $k_a$  the spring constant and  $B_a$  the damper constant. The displacement of the CoM is small enough to assume  $\sin\theta = \theta$ . Then, Eq. (7) becomes:

$$\tau = -ml^2\ddot{\theta}(t) - B_a l\dot{\theta}(t) - k_a l\theta(t) + mgl\theta(t) \quad (8)$$

Torque can be also obtained from the ZMP measurement as:

$$\tau = -x_{FT} \cdot mg \quad (9)$$

where  $x_{FT}$  is the measured ZMP from the sensors. Combining both equations we obtain:

$$-ml^2\ddot{\theta}(t) - B_a l\dot{\theta}(t) - k_a l\theta(t) + mgl\theta(t) = -x_{FT}(t)mg \quad (10)$$

Finally, the transfer function obtained from Eq. (10) is:

$$\frac{\Theta(S)}{X(S)} = \frac{\gamma}{S^2 + \alpha S + \beta} \quad (11)$$

where  $\gamma = g/l^2$ ,  $\alpha = B_a/ml$ , and  $\beta = (K_a - g)/l$ . In the steady state, when time goes to infinity, the DC gain of the system is represented by Eq. (12), that only depends on the  $K_a$  parameter. This one is in charge of eliminate the static error.

$$K_{DC} = \frac{\gamma}{\beta} \quad (12)$$

#### 4.3. Steady state ZMP error characterization

The next step is to characterize the deviation of the ZMP. Even though ankle position control succeed the ZMP measurement presents deviations. This means that the angular controller of the ankle joint works properly but the measured ZMP value has a deviation from the planed or expected value. From trials dataset depicted in Fig. 14, the deviation of the ZMP can be determined. Fig. 16 represents this deviation of the  $ZMP_{F-T}$  (output) from the  $ZMP_{ref}$  (input). The relation between the expected ZMP value and the measured one should be linear but the figure demonstrate that the real values don't match with the expectation.

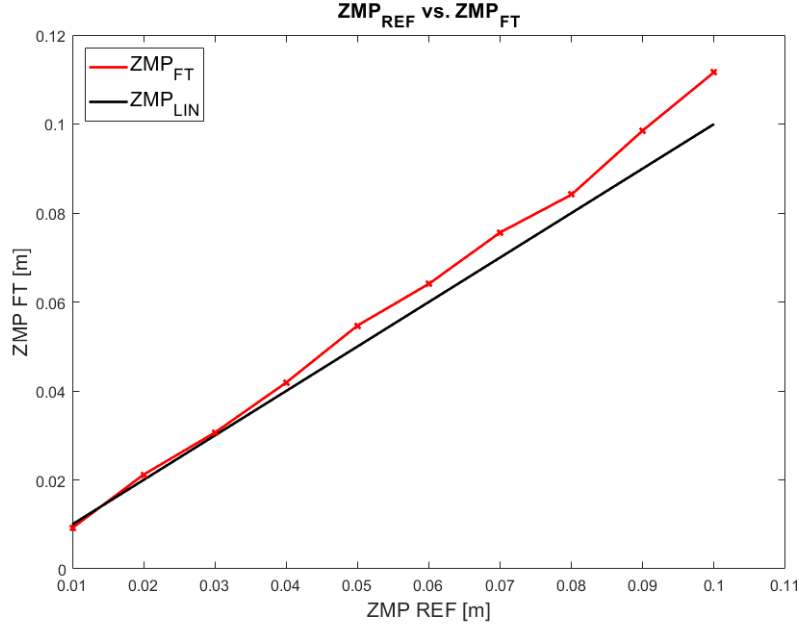


**Figure 16.** Experimental  $ZMP_{ref} - ZMP_{F-T}$  steady state values comparison.

The deviation in each test point is used to fit it to a second order polynomial Eq. (13). This equation represents the real ZMP  $x_{F-T}$  measured by the ankle sensors:

$$x_{F-T} = a \cdot x_{ref}^2 + b \cdot x_{ref} + c \quad (13)$$

where  $a = 0.834$ ,  $b = 1.024$  and  $c = -0.0004$ .

This equation represents the steady state error of the open-loop system for each working point. Eq. (12) and Eq. (13) are the base for planing the evolution of the joint angle and, therefore, ZMP location. Once the static error has been minimized the transient response must be optimized to reduce the level of oscillations.

#### 4.4. ZMP transient response characterization

Linear inverted pendulum is inherently unstable. It is necessary to develop a controller to stabilize it against any kind of disturbance. Meanwhile the angular response of the inverted pendulum goes to infinite, higher order systems can present stable behaviors. Fig. 17 shows the comparison of the LIPM vs. DLIPM transfer functions response to a simulated step perturbation. This behavior also means that the dynamic parameters can be adjusted to higher values in the DLIPM case than in a controller including the LIPM model, having more margin of adjustment.

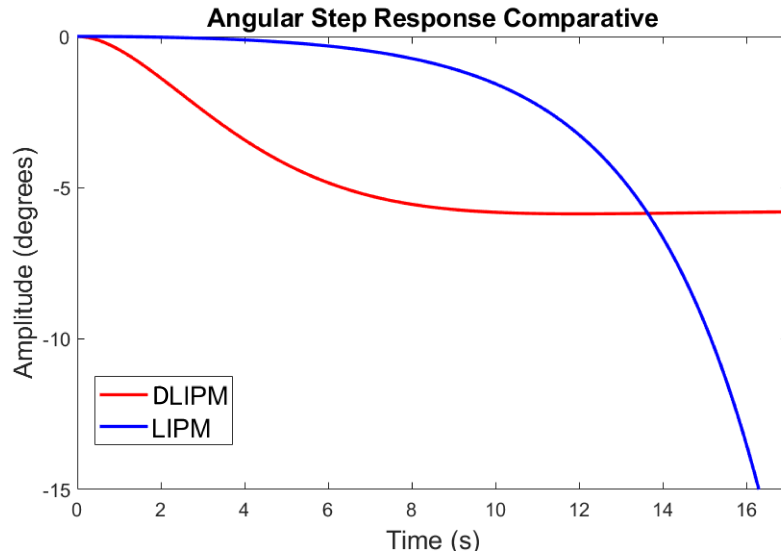


Figure 17. Angular step response LIPM-DLIPM.

301 The behavior of the humanoid robot system acting like an inverted pendulum has been  
 302 demonstrated as a under damped system. Selecting appropriate gain and dynamic parameters  
 303 it is possible manipulate the overall response of the system, reducing the over shooting and oscillation  
 304 of the system. ZMP oscillations have higher values when its location is further from the origin and, as  
 305 well, when the input angle have a high variation. This relation between ZMP and ankle angle allows  
 306 the reduction of the oscillation level by means of angle planning. In Eq. (11), dynamic parameters can  
 307 be configured, for example, to limit the over shooting level. These dynamic parameters can be obtained  
 308 from  $\alpha$  that is related to  $B_a$ . Fig. 18 shows the signal obtained from the simulation of a disturbance  
 309 causing a ZMP variation of 9cm. The dynamic parameters were designed to obtain an over damped  
 310 response ( $\zeta = 0.8$ ,  $\omega_n = 0.4376$ ).

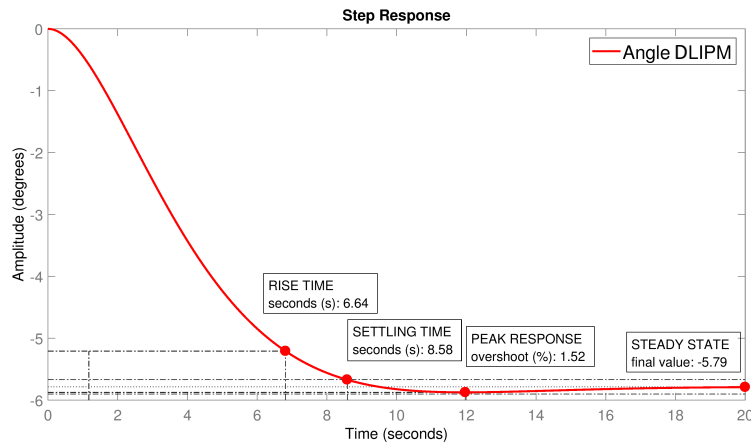


Figure 18. Angular step response DLIPM.

311 Then, selecting the proper parameters it is possible to modulate the dynamics of the robot and  
 312 reduce undesired oscillation levels on the robot.

#### 313 4.5. ZMP control

314 Classical control architectures, such as the one shown in Fig. 9, are based the linearized controller  
 315 around a working point. It means that the controller is has almost no error in this working point and

it has more error as the control target is further than this point. In this work, a non-linear solution is proposed, based on the *Gain Scheduled Matching*. The main goal is to select dynamically the most appropriate parameters for multiple working points of the controller. That is, the dynamics of the DLIPM model depends on the actual behavior of the robot and not on pre-computed static parameters. In control theory, a gain-scheduled controller is a system control architecture in which its gains are automatically adjusted as a function of time, operating condition, or plant parameters [16]. Gain scheduling is a common strategy for controlling systems in which its dynamics change with such variables. Typically, gain-scheduled controllers are fixed single loop or multi-loop control structures that use lookup tables to specify gain values as a function of the scheduling variables. For tuning purposes, it is convenient to replace lookup tables with parametric gain surfaces, such as fuzzy surfaces [25][26]. A parametric gain surface is a basis function expansion in which its coefficients are tunable. For applications where gains vary smoothly with the scheduling variables, this approach lets tune a few coefficients rather than many individual lookup-table entries, drastically reducing the number of parameters. This approach also provides explicit formulas for the gains, and ensures smooth transitions between operating points.

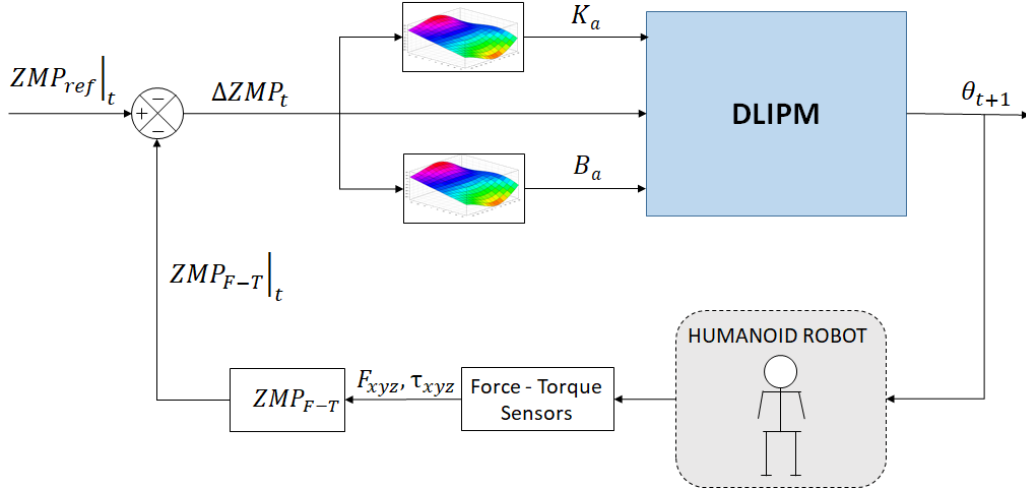


**Figure 19.** TEO ZMP controller.

The control architecture is presented in Fig. 19, similar to the human-inspired control architecture presented in [27]. In this case, there is a preprocessing module for control parameters planning. Depending on the input  $u$  the appropriate values for  $K_a$  and  $B_a$  can be selected. Then, these parameters are used for computing the values of the coefficients of the DLIPM' transfer function. These parameters customize and modify, for each control state, the dynamics of the DLIPM model. Finally, the DLIPM module outputs the ankle angle to be commanded to the robot. The angular transition is in this case smoother than the one obtained with other approaches.

#### 4.6. Experimental validation

To check the feasibility of the proposed system, it was tested experimentally performing a set of trials for capturing the response of the control system against a variation on the ZMP target. The DLIPM state space model was customized with the parameters for each ZMP target, following the step pattern. Then, the output of the model was the customized angle commands following the ZMP planning. Table 1 shows numeric result of ZMP location, comparing the values obtained from the classical approach and the DLIPM approach. It can be observed that the static error is reduced in each working point. Even in the most critical ZMP location ( $ZMP = 10cm$ ), the error has been



reduced in more than 80 % between the obtained ZMP measurements using the classical LIPM and the compensated model proposed in this paper.

**Table 1.** ZMP comparison using LIPM and DLIPM.

$ZMP_{REF}$ [m]	$ZMP_{F-T}$ [m]			
	LIPM model	% error	DLIPM model	% error
0.00	$5 \cdot 10^{-5}$	0.0	$2 \cdot 10^{-7}$	0.0
0.01	0.0092	8.2	0.0100	0.0
0.02	0.0211	6.0	0.0201	0.5
0.03	0.0306	2.2	0.0310	3.3
0.04	0.0419	4.8	0.0412	3.0
0.05	0.0547	9.4	0.0512	2.4
0.06	0.0641	6.8	0.0620	3.3
0.07	0.0756	8.0	0.0714	2.0
0.08	0.0841	5.2	0.0816	2.0
0.09	0.0902	9.5	0.0989	0.2
0.10	0.1116	11.6	0.1020	2.0

Data from Table 1 has been depicted in Fig. 20. It can be observed that the error in the classical system is higher when the ZMP location is further from the initial zero position ( $ZMP_{LIPM}$ ). Furthermore, the DLIPM curve ( $ZMP_{DLIPM}$ ) is more adjusted to the desired linear response ( $ZMP_{LIN}$ ).

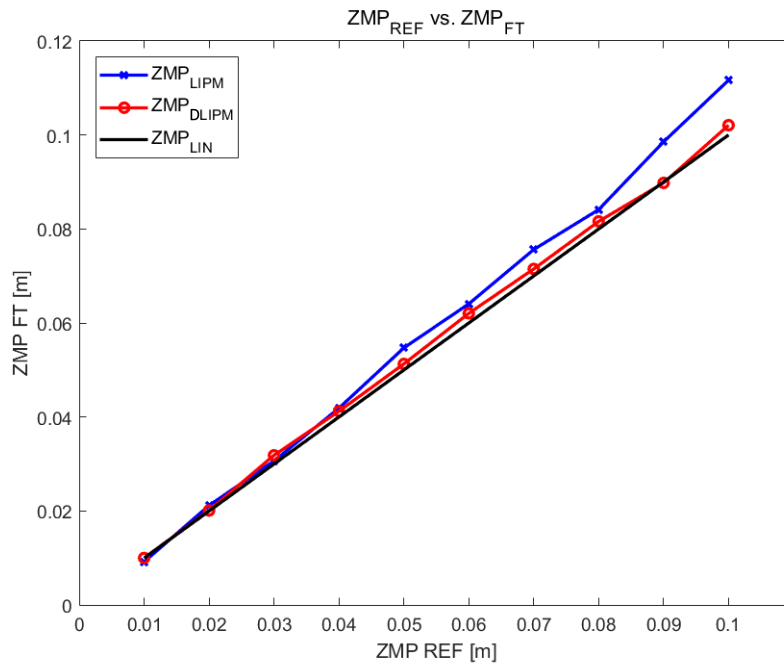
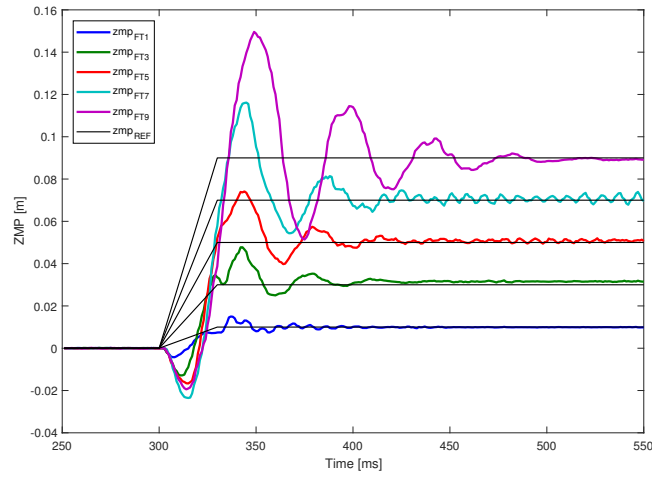
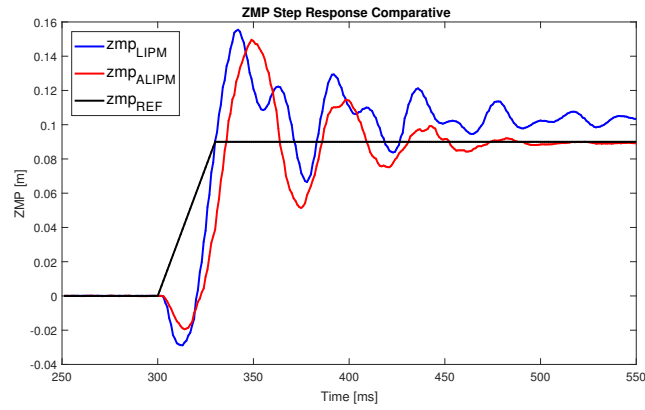


**Figure 20.** ZMP comparison using LIPM and DLIMP.

About the dynamic response of the system, Fig. 21 depicts the results from all the trials performed. Comparing this figure with Fig. 14, it is easy to observe that the level and the duration of oscillations has been reduced. Although, the over shooting has similar levels in some experiments, the state of the robot is stabilized in general earlier than the classical architecture.



(a) Step response experiments on DLIPM.



(b) Comparative between LIPM-DLIPM for ZMP = 9 cm.

**Figure 21.** ZMP step responses comparative.

## 5. CONCLUSIONS AND FUTURE WORKS

Humanoid balance control is based on the knowledge of certain equilibrium indicators. These parameters are materialized in mathematical models that represent simplifications of the humanoid body behavior. The less simplified is the model, the more accurate is the control performance but then computational complexity is higher. Classical simplified models, such as the LIPM, have a high level of simplification. It can model the walking behavior and balance but, as well, introduce approximation errors. On the other hand, the robot mechanics and electronics have inherent inaccuracies that are added to those from the model. This work has presented one method to modify the humanoid robot model to reduce these inaccuracies and to improve the balance control system. The experimental procedure, founded in push-recovery trials, has been used to determine the steady state error and the dynamic response of the system. This procedure can be applied to any kind of humanoid robot because is independent of the system and it is able to characterize any kind of inaccuracy.

The resulting model, name here as DLIPM, is the base to implement a model-based balance controller. Linear balance controllers based on the use of these simplified models need a very precise and complex tuning to find the optimal control parameters. Furthermore, these kind of controllers are designed to operate around a working point with a minimum error. Nevertheless, the balance architecture proposed, using the DLIPM, has been conceived to operate in multiple working points, minimizing the error in each one. The DLIPM is a template that must be fulfilled with the proper

parameters for each specific working point, which is related to the balance status of the robot (ZMP). These parameters define two things: the evolution of the ZMP between two consecutive postures and the level of error in each ZMP. In the first case, it has been achieved a smoother trajectory between postures reducing undesired oscillations, especially in critical ZMP locations. In the second case, the error between desired ZMP location and the measured ZMP has been reduced. These results are shown in Table 1.

Currently, the described work deals with the humanoid robot modeling in a laboratory environment with flat surfaces. The next step is to extend the procedure to models applied to other robot behaviors, such as walking in uneven surfaces. Moreover, new improvements are need to evaluate the influence of the upper body movement or the behavior of the control system when carrying objects.

## ACKNOWLEDGMENT

The research leading to these results has received funding from the RoboCity2030-III-CM project (Robótica aplicada a la mejora de la calidad de vida de los ciudadanos. fase III; S2013/MIT-2748), funded by Programas de Actividades I+D en la Comunidad de Madrid and cofunded by Structural Funds of the EU. We would like to thank Maria Dolores Pinel and Aitor Gonzalez for their collaboration during the experimental and data processing phases.

## References

1. Henze, B.; Dietrich, A.; Ott, C. An approach to combine balancing with hierarchical whole-body control for legged humanoid robots. *IEEE Robotics and Automation Letters* **2016**, *1*, 700–707.
2. Morisawa, M.; Kita, N.; Nakaoka, S.; Kaneko, K.; Kajita, S.; Kanehiro, F. Biped locomotion control for uneven terrain with narrow support region. *System Integration (SII), 2014 IEEE/SICE International Symposium on* **2014**, pp. 34–39.
3. Budiharto, W.; Moniaga, J.; Aulia, M.; Aulia, A. A framework for obstacles avoidance of humanoid robot using stereo vision. *International Journal of Advanced Robotic Systems* **2013**, *10*, 204.
4. McGill, S.G.; Zhang, Y.; Vadakedathu, L.; Sreekumar, A.; Yi, S.J.; Lee, D.D. Comparison of Obstacle Avoidance Behaviors for a Humanoid Robot in Real and Simulated Environments. *Humanoid Robots, 2012. IEEE International Conference on* **2012**.
5. Arbulu, M.; Balaguer, C. Real-time gait planning for the humanoid robot Rh-1 using the local axis gait algorithm. *International Journal of Humanoid Robotics* **2009**, *6*.
6. Stephens, B. Humanoid push recovery. *Humanoid Robots, 2007 7th IEEE-RAS International Conference on* **2007**, pp. 589–595.
7. Yun, S.k.; Goswami, A.; Sakagami, Y. Safe fall: Humanoid robot fall direction change through intelligent stepping and inertia shaping. *2009 IEEE International Conference on Robotics and Automation* **2009**, pp. 781–787.
8. Agravante, D.J.; Sherikov, A.; Wieber, P.B.; Cherubini, A.; Kheddar, A. Walking pattern generators designed for physical collaboration. *Robotics and Automation (ICRA), 2016 IEEE International Conference on* **2016**, pp. 1573–1578.
9. Yin, C. Walking Stability of a Humanoid Robot Based on Fictitious Zero-Moment Point. *Power Engineering* **2006**, pp. 1–6.
10. Lee, S.H.; Goswami, A. The reaction mass pendulum (RMP) model for humanoid robot gait and balance control. In *Humanoid Robots*, First ed.; Choi, B., Ed.; InTech, 2009; Vol. 71, pp. 169–186.
11. Feng, S.; Sun, Z. Biped Robot Walking Using Three-Mass Linear **2008**. pp. 371–380.
12. González-Fierro, M.; Monje, C.; Balaguer, C. Fractional Control of a Humanoid Robot Reduced Model with Model Disturbances. *Cybernetics and Systems* **2016**, *47*.
13. Martínez, S.; Monje, C.A.; Jardón, A.; Pierro, P.; Balaguer, C.; Muñoz, D. TEO: Full-Size Humanoid Robot Design Powered by a Fuel Cell System. *Cybernetics and Systems* **2012**, *43*, 163–180.

14. Kajita, S.; Hirukawa, H.; Harada, K.; Yokoi, K. Introduction to Humanoid Robotics. In *Springer Tracts in Advanced Robotics*; Siciliano, B.; Khatib, O., Eds.; Springer-Verlag Berlin Heidelberg: Berlin, Heidelberg, 2014; Vol. 101.
15. Kajita, S.; Kanehiro, F.; Kaneko, K.; Yokoi, K.; Hirukawa, H. The 3D linear inverted pendulum mode: a simple modeling for a biped walking pattern generation. *Proceedings 2001 IEEE/RSJ International Conference on Intelligent Robots and Systems*; IEEE: Maui, 2001; Vol. 1, pp. 239–246.
16. Kljuno, E.; Williams, R.L. Humanoid Walking Robot: Modeling, Inverse Dynamics, and Gain Scheduling Control. *Journal of Robotics* **2010**, 2010.
17. Feng, S.; Sun, Z. Biped robot walking using three-mass linear inverted pendulum model. In *International Conference on Intelligent Robotics and Applications*; Xiong, C.; Huang, Y., Eds.; Springer Berlin Heidelberg: Berlin, Heidelberg, 2008; pp. 371–380.
18. Vukobratovic, M.; Borovac, B. Zero-moment point — thirty five years of its life. *International Journal of Humanoid Robotics* **2004**, 1, 157–173.
19. Kajita, S.; Kanehiro, F.; Kaneko, K.; Fujiwara, K.; Harada, K.; Yokoi, K.; Hirukawa, H. Biped walking pattern generation by using preview control of zero-moment point. *Proceedings of the 2003 IEEE International Conference on Robotics and Automation*; IEEE: Taipei, Taiwan, 2003; pp. 1620–1626.
20. Nenchev, D.N.; Nishio, A. Ankle and hip strategies for balance recovery of a biped subjected to an impact. *Robotica* **2008**, 26, 643–653.
21. Kajita, S.; Yokoi, K.; Saigo, M.; Tanie, K. Balancing a humanoid robot using backdrive concerned torque control and direct angular momentum feedback. *Robotics and Automation, 2001. Proceedings 2001 ICRA. IEEE International Conference on* **2001**, 4, 3376–3382.
22. Kim, J.H.; Oh, J.H. Walking control of the humanoid platform KHR-1 based on torque feedback control. *IEEE International Conference on Robotics and Automation, 2004. Proceedings. ICRA '04. 2004* **2004**, 1, 623–628.
23. Kaynov, D. Open motion control architecture for humanoid robots. PhD thesis, University Carlos III of Madrid, 2009.
24. Ogata, K.; Yang, Y. Modern control engineering; Prentice-Hall Englewood Cliffs, NJ: Upper Saddle River, New Jersey, 1970.
25. Safiotti, A. Fuzzy logic in autonomous robotics: behavior coordination. *Proceedings of 6th International Fuzzy Systems Conference* **1997**, 1, 573–578.
26. Takagi, T.; Sugeno, M. Fuzzy identification of systems and its applications to modeling and control. *IEEE Transactions On Systems Man And Cybernetics* **1985**, 15, 116–132.
27. Martínez de la Casa Díaz, S. Human inspired humanoid robot control architecture. PhD thesis, University Carlos III of Madrid, 2012.